M&C 2001 Salt Lake City, Utah, USA, September 2001.

CHARACTERIZATION OF NEUTRON EMISSION FROM A D-D FILLED PLASMA FOCUS

Federico Rocchi and Marco Sumini

INFM-BO and Laboratorio di Montecuccolino,
Dipartimento di Ingegneria Energetica, Nucleare e del Controllo Ambientale,
Faculty of Engineering, Bologna University
Via dei Colli 16, 40136 Bologna, ITALY
federico.rocchi@mail.ing.unibo.it marco.sumini@mail.ing.unibo.it

Keywords: Plasma Focus, neutron spectra, beam-target model

ABSTRACT

The theoretical characterization with respect to energy and angle of the neutrons emitted in a plasma focus device discharge is reviewed and analyzed and some preliminary results are presented and discussed.

1. INTRODUCTION

The relevance and importance of a plasma focus (PF) device (Mather, 1971; Cloth, 1977; Nardi, 1992) as intense source of neutrons are due essentially to the low costs and dimensions of the device itself, to its high performances in terms of neutrons emitted per discharge and to the type of spectra of the emitted neutrons. For instance a D-T filled advanced plasma focus (APF) (Nardi, 1992) with a capacitor bank energy of about 200 KJ can give about 10^{14} neutrons per discharge, these being emitted almost pointwisely and almost monoenergetically at about 14 MeV. If moreover the advanced plasma focus is repetitive so that the number of discharges per unit time allows frequent neutron emissions, the device can be considered a continuous neutron source. The main technological problems are indeed related to the stability of the discharge repetition rates, which nowadays can reach 10-15 Hz and can be sustained for times of the order of magnitude of the hour. If the technology related to these performances could be improved somehow, PF devices will be highly competitive as neutron sources in the future.

If these devices are to be used in many kinds of applications as intense neutron sources, great theoretical and experimental (f.i. Steinmetz, 1982) efforts should be directed towards a better characterization of the energetic and angular distribution of the emitted neutrons, in other words towards a better characterization of the neutronics of PF machines. This means that fusion doubly-differential cross sections are to be more correctly evaluated, and the models giving the corresponding fusion reaction rates more precisely set-up, as well as the description of the intrinsic plasma dynamics in the pinch zone of the PF.

Presently two main classes of models for the evaluation of fusion reaction rates are used, the “beam-target” one and the “Maxwellian reactivity” one. The beam-target model was introduced by Bernstein and Comisar in the late ‘60s and early ‘70s and it is presently the most largely accepted. This model assumes that the colliding ions in the pinch zone of the PF can be divided into two sub-populations of “beam ions” and “target ions”. The target ions are assumed in many calculations to be at rest; axially only moving target ions have also been considered and the comparison between theoretical calculations and experimental results has shown (Bernstein, 1972; Tiseanu, 1994) that there was not an appreciable improvement with respect to the model which assumes target ions at rest. The fusion reactions are assumed to happen in so a small zone of the pinch area that a spatial description of the problem is unessential. Reaction rates are then calculated as being the production term of the collision term of the Boltzmann equation for the interaction of the two sub-populations. In doing this, one has to know the energetic and angular dependence of the beam ions distribution function. Bernstein and Comisar (1972) were the first to perform beam-target reactivity calculations assuming energetic and angular dependencies for the beam ions distribution functions which were dictated by a few experimental studies and by the common-sense of the authors. In more recent years there has been a lot of efforts both in the direction of theoretically evaluating the beam ions distribution function and in that of experimentally determining the emitted neutrons distribution. The consistence of these results has been checked using the beam-target model, and considerable improvements have been made since the times of Bernstein and Comisar. However in even more recent times new and highly improved cross-section data have been made available (see below) and so it would be important to repeat the calculations by Bernstein and Comisar using these new data and the new features which have been discovered meanwhile about the beam ions distribution function.

In this paper doubly-differential neutron emission reaction rates have been calculated for a D-D filled Mather-type PF at low deuteron energies (40-100 KeV), taking into account recent and improved cross-section data and new beam ions distribution functions.

2. MODEL EQUATIONS

By definition the reaction rate R for reaction i in a space independent problem is given by

$$R = n_D n_T \int_{4\pi}\int_{\Re^3}\int_{\Re^3} f\left(\vec{v}_D\right) F\left(\vec{v}_T\right) g \frac{d\sigma_i}{d\Omega} d\Omega\, d\vec{v}_D\, d\vec{v}_T \tag{1}$$

where n_D and n_T are the beam and target ions densities with unit-normalized distribution functions f and F respectively; g is the modulus of the relative velocity between beam and target ions and $\frac{d\sigma_i}{d\Omega}$ is the doubly-differential cross section. In the Bernstein-Comisar formalism one can introduce the dummy variable E by use of a Dirac Delta distribution, so that

$$R(E)=n_D n_T \int\limits_{4\pi}\int\limits_{\Re^3}\int\limits_{\Re^3} f(\vec{v}_D)F(\vec{v}_T)g\frac{d\sigma_i}{d\Omega}\delta(E-E_n)\,d\Omega\,d\vec{v}_D\,d\vec{v}_T\,dE \tag{2}$$

where E_n is the emitted neutron energy. This is given, in the case of axially moving target ions, by the laws of energy and momentum conservation in the binary D-D reaction as (Bernstein, 1972; Tiseanu, 1994):

$$E_n = W_n\left(1+\gamma^2+2\gamma\cos\psi_n\right) \tag{3}$$

where

$$W_n = \frac{3}{4}\left(Q+\frac{E_B}{2}\right)=2.45+\frac{3}{8}E_B \quad \text{MeV} \quad \text{and} \tag{4}$$

$$Q=3.25 \quad \text{MeV} \tag{5}$$

is the Q-value of the fusion reaction D+D→He^3+n. E_B is the deuteron bombarding energy, related to the beam deuteron kinetic energy E_D by

$$E_B = E_D\left(1+\rho^2-2\rho\cos\vartheta_D\right) \tag{6}$$

where $\rho=\left|\frac{v_T}{v_D}\right|$ is the ratio between the target and beam ions speeds. Also

$$\cos\psi_n = -\gamma\, sin(\psi_L)^2+\cos\psi_L\sqrt{1-\gamma^2 sin(\psi_L)^2} \tag{7}$$

$$\cos\psi_L = \cos\vartheta_n\cos\vartheta_{cm}+sin\,\vartheta_n sin\,\vartheta_{cm}\cos\varphi \tag{8}$$

$$\tan\vartheta_{cm} = \frac{sin\,\vartheta_D}{\cos\vartheta_D+\rho} \tag{9}$$

$$\gamma=\sqrt{\frac{E_{cm}}{2W_n}} \tag{10}$$

$$E_{cm} = \frac{1}{4}E_D\left(1+\rho^2+2\rho\cos\vartheta_D\right) \tag{11}$$

where ψ_L is the angle between the deuteron center-of-mass velocity and the emitted neutron velocity in the laboratory system, ψ_n is the neutron emission angle in the center of mass system, ϑ_D is the colliding deuteron angle in the laboratory system, ϑ_n is the neutron emission angle in the laboratory system, E_{cm} is the bombarding deuteron kinetic energy in the center of mass system and ϑ_{cm} is the deuteron angle in the center of mass system. Laboratory system angles are measured with respect to the PF axis. In what follows it will be assumed that target ions are at rest instead of being axially moving. In this way eq.s (3) to (11) simplify because $\rho = 0$. Fig.1 shows the velocity vectors for the case of target ions at rest.

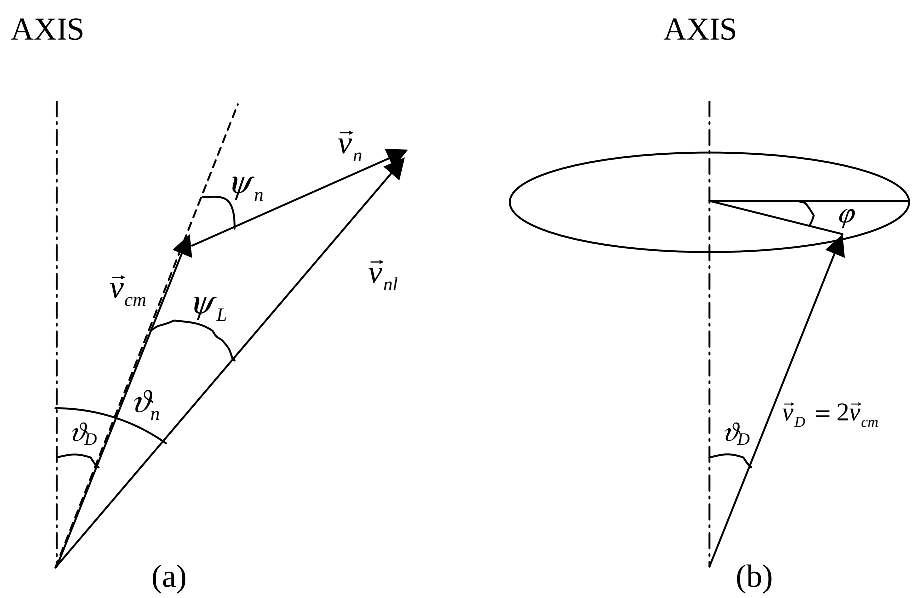

Fig. 1 Vector diagrams for beam-target fusion collisions; (a): off-axis deuteron incident upon stationary target ion; (b): neutron emitted in center of mass and laboratory systems.

The doubly-differential neutron emission reaction rate is thus obtained from eq. (2) as:

$$\frac{d^2R(E,\vartheta_n)}{dEd\Omega} = n_D n_T \int_{\Re^3}\int_{\Re^3} f(\vec{v}_D)F(\vec{v}_T)g\frac{d\sigma_i}{d\Omega}\delta(E-E_n)d\vec{v}_D\,d\vec{v}_T\,. \tag{12}$$

In the case of target ions at rest, the integration of the target ions distribution function is obviously normalized to one, so that, after a change of variables,

$$\frac{d^2R(E,\vartheta_n)}{dEd\Omega} = n_D n_T \int_0^{2\pi}\int_0^{\pi}\int_0^{+\infty} f(E_D,\vartheta_D)g\frac{d\sigma_i}{d\Omega}\delta(E-E_n(\vartheta_D,\varphi,E_D))\cdot$$
$$\cdot\sqrt{\frac{2E_D}{m_D^3}}\,dE_D\sin\vartheta_D d\vartheta_D d\varphi. \tag{13}$$

It must be stressed here that E_n , for fixed E_D , is a non-linear function of ϑ_D and φ and that the beam ions distribution function can be assumed independent of φ. Moreover it is important to realize that, due to energy and momentum conservation, the non-linear function E_n has global minimum and maximum for every given value of E_D.

3. BEAM IONS DISTRIBUTION FUNCTION

The particular form of the angle dependence of the reacting beam ions distribution function is not well known, and in general a separation of angular from energetic variables for f is not even possible. In many cases however a separation of variables has been made and the energetic part of the beam ions distribution function has been assumed (Bernstein, 1972; Stygar, 1982) to follow a particular power law of the form $E_D^{-\alpha}$. The parameter α can be estimated experimentally in various ways; Bernstein and Comisar (1972) proposed two possible values, 2 and 3 respectively, valid for deuteron energies from about 50 to about 400 KeV. More recent investigations (Stygar, 1982) have shown that a suitable value is 3.5±0.5. For low deuteron energies in the range from 40 to 100 KeV Tiseanu, Mandache and Zambreanu (1994) showed that the beam ions distribution function is so narrow in energy that it can be estimated to follow a Dirac distribution of the form $\delta(E_D - E_{D0})$ where E_{D0} can be considered as the mean value of the energy. In the same energy range they also proposed a Gaussian-shaped profile for the angular dependence of f with an ad hoc half-width at half-maximum. This profile can then be transformed in an easier expression by a Taylor series expansion so that one has, apart from a normalization factor:

$$f(E_D, \vartheta_D) \propto \delta(E_D - E_{D0}) e^{-\frac{1-\cos\vartheta_D}{2(1-\cos\vartheta_{D0})}} \tag{14}$$

where ϑ_{D0} is a parameter that in the low energy range is taken equal to $\frac{\pi}{6}$. With this form of distribution function eq. (13) becomes:

$$\frac{d^2R(E,\vartheta_n)}{dEd\Omega} = \Theta \int_0^{2\pi}\int_0^{\pi} e^{-\frac{1-\cos\vartheta_D}{2(1-\cos\vartheta_{D0})}} \frac{d\sigma_i(\vartheta_D,\varphi,E_{D0})}{d\Omega} \delta(E - E_{n0}(\vartheta_D,\varphi)) \cdot$$
$$\cdot \sin\vartheta_D d\vartheta_D d\varphi = \Theta \int_0^{2\pi}\int_0^{\pi} G(\vartheta_D,\varphi) \delta(E - E_{n0}(\vartheta_D,\varphi)) d\vartheta_D d\varphi = \Theta H(E,\vartheta_n) \tag{15}$$

where

$$E_{n0}(\vartheta_D,\varphi) = E_n(\vartheta_D,\varphi,E_{D0}) \quad \text{and} \tag{16}$$

$$\Theta = \xi \, n_D \, n_T \; g(E_{D0}) \sqrt{\frac{2E_{D0}}{m_D^3}} \tag{17}$$

with ξ normalization factor for *f*. The integrand function *G* is such that

$$G(0,\varphi) = G(\pi,\varphi) = 0\,. \tag{18}$$

In order to numerically evaluate eq. (15) it is necessary to know the energy and angle expression of the D-D fusion cross section.

4. REACTION CROSS SECTION

Two possible fusion reactions are involved when two deuterons collide:

$$D+D \rightarrow He^3+n \tag{19}$$

$$D+D \rightarrow T+p. \tag{20}$$

Only reaction eq. (19) is of interest for the production of neutrons; the chance of happening of the two reaction is about 50% - 50%. The reference data used by Bernstein and Comisar for the doubly differential cross section of reaction eq. (19) were those published by Theus, McGarry and Beach (1966). Only recently (1990) however it became apparent that the published data were not correct, due to some computational errors. These errors produced results that were affected in certain cases by uncertainties of 10-20%. At the beginning of the ‘90s the Los Alamos program in Low-Energy Fusion Cross Sections (LEFCS) produced extremely accurate data (Brown, 1990) for reaction eq. (19), but the given angular dependence is valid only from 20 to about 120 KeV, though the energy one is quite well-known up to the MeV region; this angle-integrated energy dependence has been included in the appropriate ENDF-B IV file, available through the FENDL/C-2.0 data library. Between the data published by Theus, McGarry and Beach and those published by Jarmie and Brown (1990) it has been available a data set of somehow intermediate accuracy given by Drosg and Schwerer (1987), which however gave the angular dependence up to the MeV region and beyond. In this paper, since the attention is focalized to the low energy region from 40 to 100 KeV, the most accurate data available, those by Jarmie and Brown, have been used. It seems that these data have never been used in the kind of calculations here presented (Mikkelsen, 1989). It must be noted however that these data are not those most recently published (Bosch, 1992).

The data by Jarmie and Brown can be cast in the following useful form:

$$\frac{d\sigma_{fus}(\Omega_{lab},E)}{d\Omega_{lab}} = \\ = \frac{\sigma_T(E)}{4\pi}\,\frac{1+A(E)\cos(\psi_n)^2+B(E)\cos(\psi_n)^4}{1+\dfrac{A(E)}{3}+\dfrac{B(E)}{5}}\,\frac{\left(1+2\gamma\cos\psi_n+\gamma^2\right)^{3/2}}{1+\gamma\cos\psi_n} \tag{21}$$

where the first factor on the rhs is the total cross section divided by the total solid angle to give an isotropic term, the second one gives the anisotropic angular dependence in the center of mass system as a kind of form factor, and the third one is a transformation term from the center of mass system to the laboratory one. For eq. (21) the following best-fittings have been computed and used (energy in eV and cross section in barns):

$$A(E)=\frac{b(E)}{a(E)} \tag{22}$$

$$B(E)=\frac{c(E)}{a(E)} \tag{23}$$

$$a(E)=a_0+a_1E+a_2E^2+a_3E^3 \tag{24}$$

$$b(E)=b_0+b_1E+b_2E^2+b_3E^3 \tag{25}$$

$$c(E)=c_0+c_1E+c_2E^2+c_3E^3 \tag{26}$$

$$\sigma_T(E)=\sigma_{T0}+\sigma_{T1}E+\sigma_{T2}E^2+\sigma_{T3}E^3+\sigma_{T4}E^4+\sigma_{T5}E^5+\sigma_{T6}E^6+\sigma_{T7}E^7 \tag{27}$$

Eq. (27) is valid up to about 600 KeV while parametrizations eq.s (22) to (27) are restricted from about 40 KeV to about 120 KeV. The coefficients are given in Table 1.

Table 1 Parametrization coefficients.

i	a_i	b_i	c_i	σ_{Ti}
0	-0.03277	-0.03281	0.05878	1.27534×10^{-4}
1	-1.52255×10^{-6}	4.70645×10^{-7}	-4.25323×10^{-6}	-6.23255×10^{-8}
2	2.20053×10^{-10}	5.13789×10^{-11}	7.94172×10^{-11}	4.225×10^{-12}
3	-9.73216×10^{-16}	-1.08306×10^{-16}	-2.09508×10^{-16}	-2.76058×10^{-17}
4				9.10543×10^{-23}
5				-1.65284×10^{-28}
6				1.56397×10^{-34}
7				-6.0193×10^{-41}

Figure 2 and 3 are plots of the total cross-section ENDF-B VI data and their fitting, and of the parameters *a*, *b* and *c* as experimental data and their fittings.

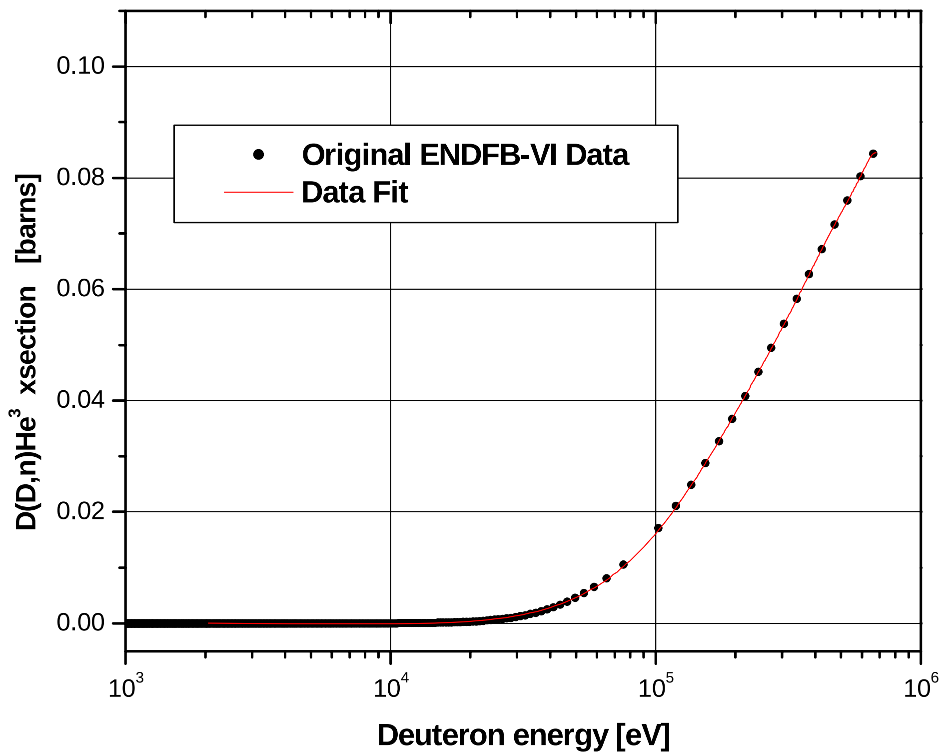

Fig. 2 Total fusion cross section for neutron production.

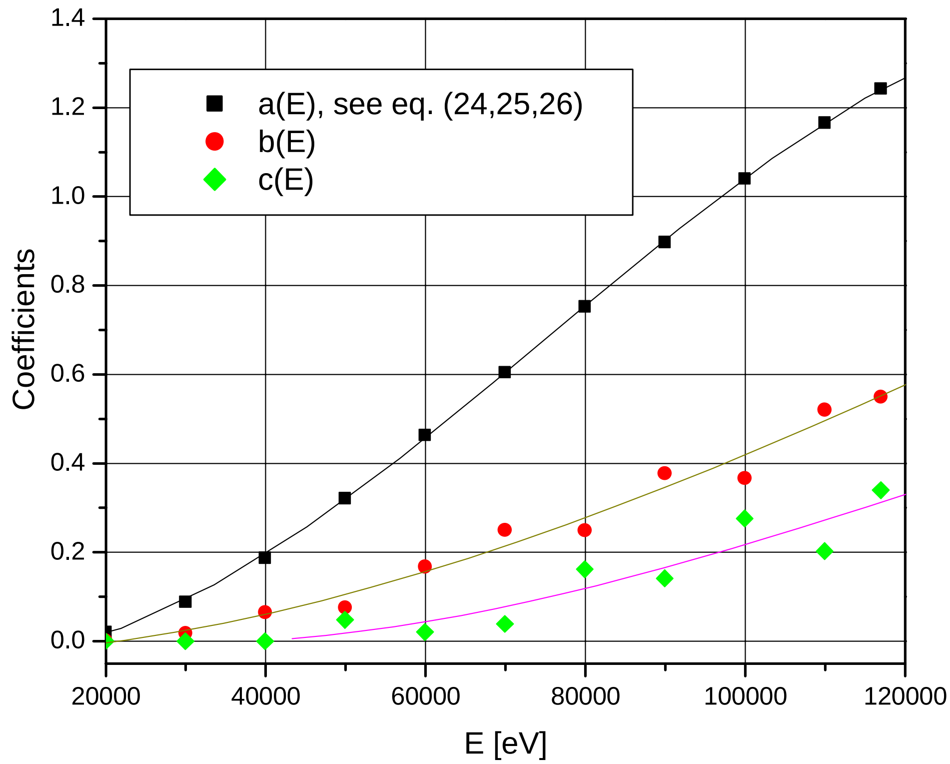

Fig.3 Parametrization coefficients: experimental data (Brown, 1990) and their fittings.

It must be noted that, for the energy range of interest of this work, only even terms in the cosine of the emission angle up to fourth order are necessary in the anisotropy form factor, because the cross section must be symmetric around $\psi_n = \pi/2$ (identity of target and projectile) and because only S, P and D waves contribute to the interaction.

5. RESULTS

Numerical integration of eq. (15) has been carried out for values of ϑ_n of 0, π/2 and π and for values of E_{D0} of 50, 70 and 90 KeV. After tedious but simple calculus manipulations, the rhs of eq. (15) can be reduced to a line integral over the contour paths given by the (ϑ_D, φ) points for which the argument of the Dirac Delta distribution vanishes, for any given values of E inside the non-denied energy intervals evaluated for each E_{D0}. An important point in the calculations is that different arguments of the Dirac Delta distribution are found for every values of ϑ_n. Fig. 4 shows the angular dependence of function E_n for $E_D = E_{D0} = 0.09$ MeV. Fig. 5 shows the integration contour paths for the same deuteron energy. Fig. 6 shows the angular dependence of G for $E_D = E_{D0} = 0.09$ MeV. Fig. 7(a,b,c) show the numerical evaluation of function H for three values of E_D and ϑ_n. These figures can be compared f.i. with those by Michel et al. (1982): while the overall behavior of the profiles is similar, there are small differences near the energy minima and maxima.

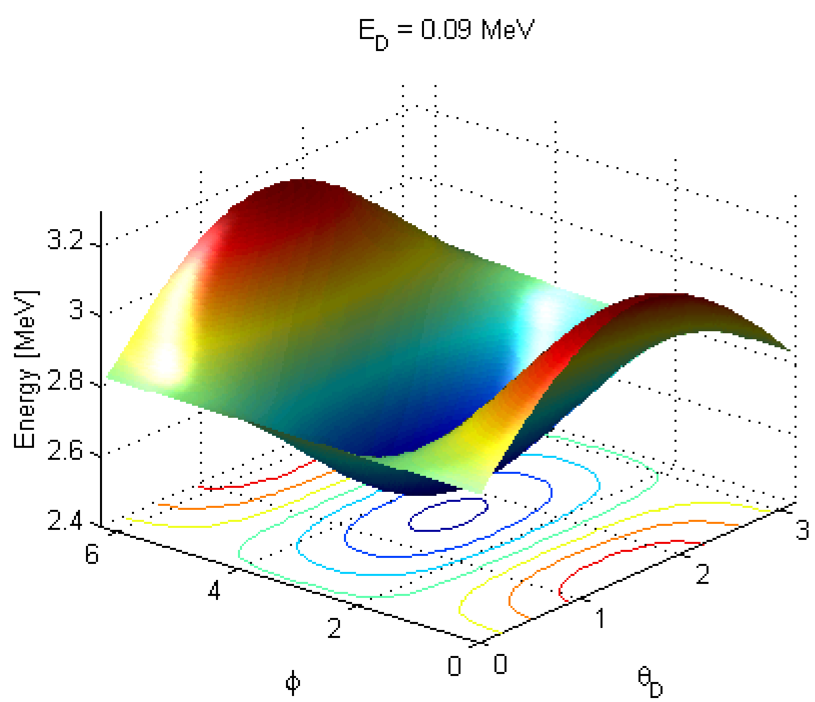

Fig. 4 Angular dependence of E_n.

The present authors think that these are due to the differences in the beam ions distribution functions which have been used; Michel et al. (1982) have used distribution functions which have a definite energy dependence and slightly different angular dependence; it must be said that also the cross section and the reaction Q-value have important roles in determining the profiles. Moreover there is not yet an agreement on the values of the normalizing factors Θ which vary with E_{D0}.

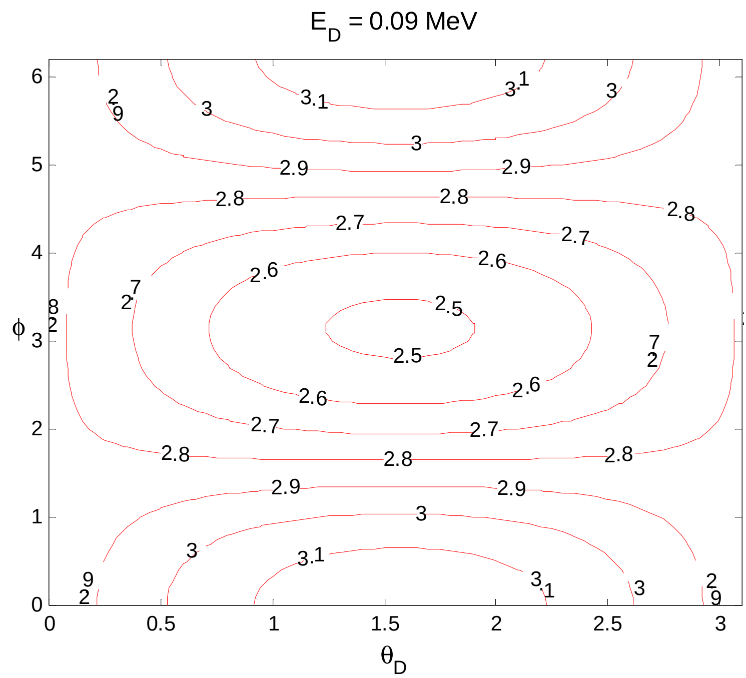

Fig. 5 Integration contour paths.

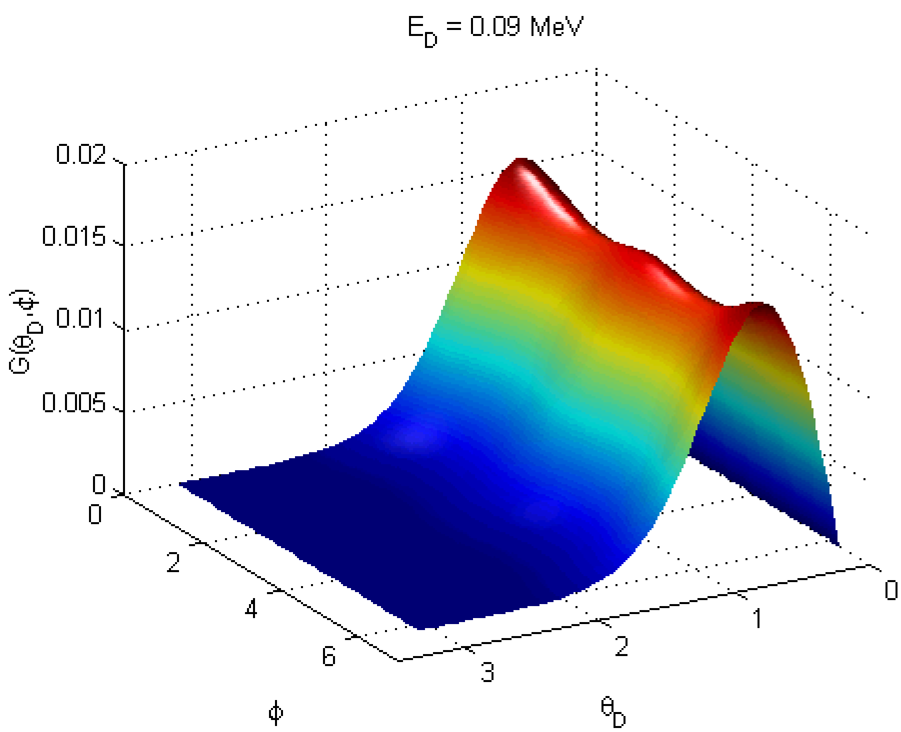

Fig. 6 $G(\vartheta_D,\varphi)$ angular dependence.

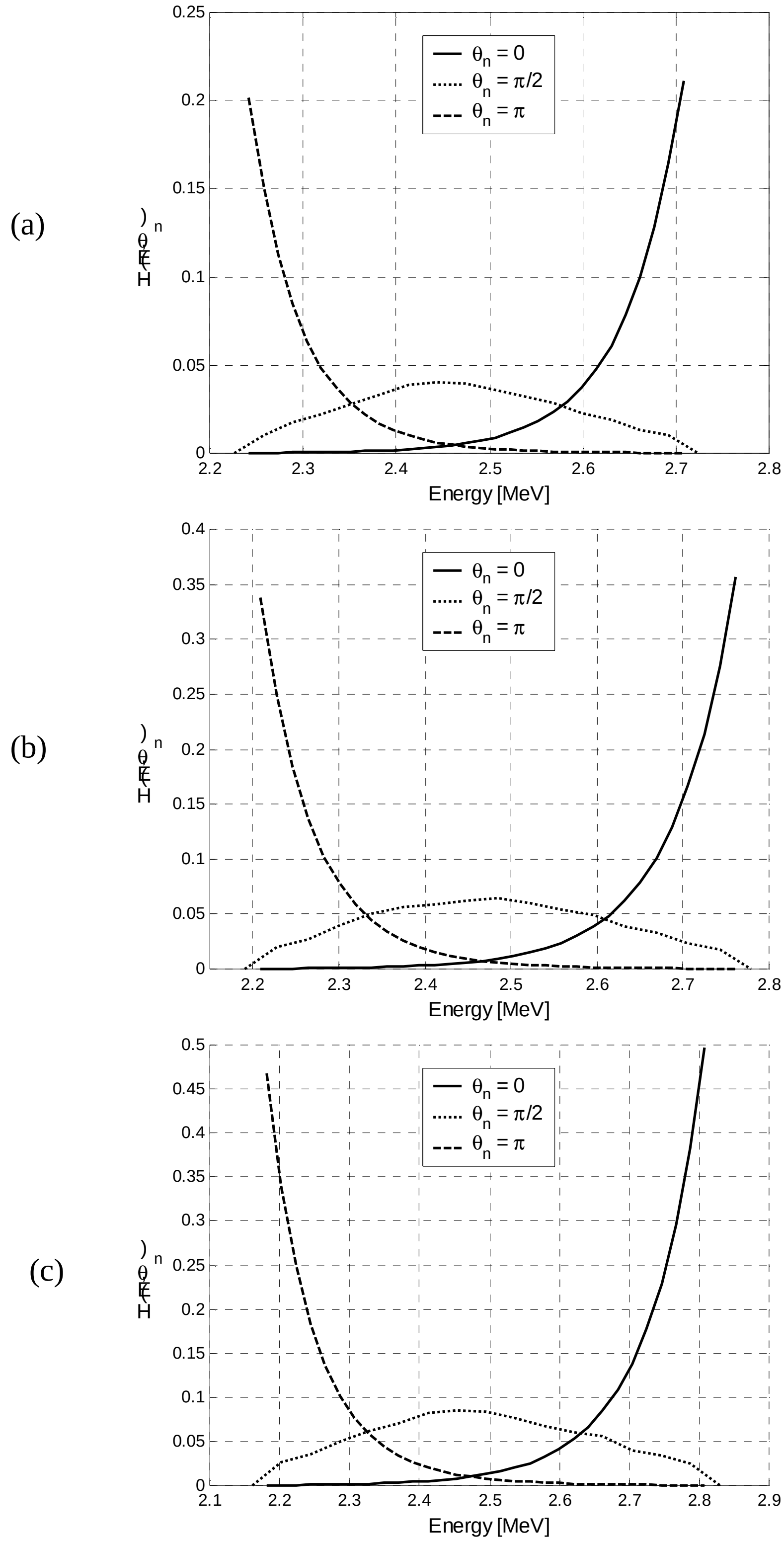

Fig. 7 *H(E,θn)* function for E_D=0.05 (a), 0.07 (b), 0.09 (c) MeV.

5. CONCLUSIONS

From the beam-target model of the D-D reactions inside a plasma focus, doubly-differential reaction rates for neutron emission have been evaluated for deuteron energies of 0.05, 0.07 and 0.09 MeV and for emission angles of 0, $\pi/2$ and π. Newer and improved cross sections have been used, as well as recently evaluated beam ions distribution functions. Slight differences in the results with respect to older calculations have been ascribed to the differences in cross sections and distribution functions. The authors feel that better theoretical and experimental estimations of these quantities may greatly improve the evaluation of emitted neutron spectra.

NOMENCLATURE

a	energy dependent anisotropy parameter
A	energy dependent anisotropy parameter
b	energy dependent anisotropy parameter
B	energy dependent anisotropy parameter
c	energy dependent anisotropy parameter
E	kinetic energy, energy, neutron energy
f	beam ion distribution function
F	target ion distribution function
g	relative velocity
G	integrand function
H	doubly-differential neutron emission reaction rate for Θ=1
n	particle number density
R	reaction rate
Q	reaction Q-value
$\vec{v}$	particle velocity
W	energy parameter
γ	energy parameter
Ω	solid angular variable
ρ	target/beam ions speed ratio
σ	microscopic cross section
$\frac{d\sigma}{d\Omega}$	doubly-differential microscopic cross section
ϑ	angular variable
Θ	normalizing factor
ψ	angular variable

Subscripts

B	bombarding particles
cm	centre of mass reference system
D	beam deuterons
$D0$	simplified beam deuterons distribution function parameter
i	nuclear reaction of type I

L laboratory system
n neutron
n0 neutron function evaluated for *D0* parameters
T target deuterons, total

Superscripts

α parameter of power law energetic dependence of beam ions distribution function

ACKNOWLEDGMENTS

The authors kindly acknowledge Sandro Manservisi, Laboratorio di Montecuccolino, for his help on certain aspects of the numerical computations, Franco Mezzetti, University of Ferrara, and Valerio Benzi, University of Bologna, for valuable discussions about PF machines, and Vincenzo Molinari, Laboratorio di Montecuccolino, for his helpful suggestions.

REFERENCES

Bernstein, M.J., Comisar, G.G., 1972. Neutron energy and flux distribution from a crossed-field acceleration model of plasma focus and z-pinch discharges. *The Physics of Fluids* **15**, 4, 700-707.

Bosch, H.S., Hale, G.M., 1992. Improved formulas for fusion cross-sections and thermal reactivities. *Nuclear Fusion* **32**, 4, 611-631.

Brown, R.E., Jarmie, N., 1990. Differential cross sections at low energies for ^{2}H(d,p)^{3}H and ^{2}H(d,n)^{3}He. *Phys. Rev. C* **41**, 4, 1391-1400.

Cloth, P., Conrads, H., 1977. Neutronics of a dense plasma focus- An investigation of a fusion plasma. *Nuclear Science and Engineering* **62**, 591-600.

Drosg, M, Schwerer, O., 1987. Production of monoenergetic neutrons between 0.1 and 23 MeV. In: *Handbook on Nuclear Activation Data*, IAEA, Vienna, pp. 83-121.

Lee, S., Tou, T.Y., Moo, S.P., Eissa, M.A., Gholap, A.V., Kwek, K.H., Mulyodrono, S., Smith, A.J., Suryadi, E., Usada, W., Zakaullah, M., 1988. A simple facility for the teaching of plasma dynamics and plasma nuclear fusion. *Am. J. Phys.* **56** (1), 62-68.

Mather, J.W., 1971. Dense plasma focus. In : *Methods of Experimental Physics*, Vol. IX, Part B, Academic Press, New York, 187-249.

Michel, L., Krompholz, H., Herziger, G., 1982. Neutron emission from a 1kJ plasma focus device. *Physics Letters* **88A**, 8, 400-402.

Mikkelsen, D.R., 1989. Approximation for non-resonant beam-target fusion reactivities. *Nuclear Fusion* **29**, 7, 1113-1115.

Nardi, V., Brzosko, J., Powell, C., 1992. Neutron sources of the advanced plasma focus type for demonstration tests of safe reactors. In: Workshop on Plasma Focus Device Utility for Intense Neutron Source Applications. Los Alamos Report LA-UR-92-3552, July 1992.

Steinmetz, K., Huebner, K., Rager, J.P., Robouch, B.V., 1982. Neutron pinhole camera investigations on temporal and spatial structures of plasma focus neutron source. *Nuclear Fusion* **22**, 1, 25-32.

Stygar, W., Gerdin, G., Venneri, F., Mandrekas, J., 1982. Particle beams generated by a 6-12.5 kJ dense plasma focus. *Nuclear Fusion* **22**, 9, 1161-1172.

Theus, R.B., McGarry, W.I., Beach, L.A., 1966. Angular distributions and cross-section ratios for the reactions $^{2}H(d,n)^{3}He$ and $^{2}H(d,p)^{3}H$ below 500 KeV. *Nucl. Phys.* **80**, 273-288.

Tiseanu, I., Mandache, N., Zambreanu, V., 1994. Energetic and angular characteristics of the reacting deuterons in a plasma focus. *Plasma Phys. Contro. Fusion* **36**, 417-432.